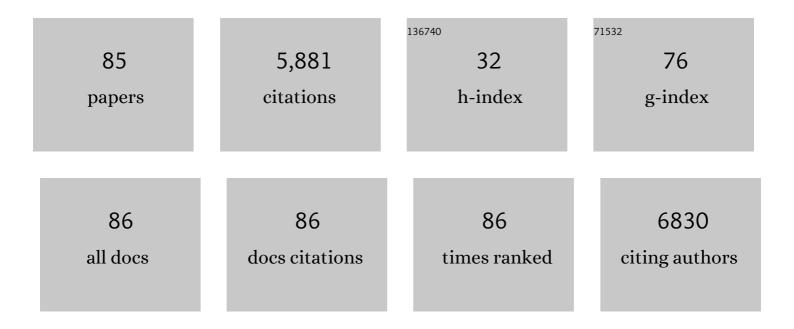
## **Daniel Spemann**

List of Publications by Year in descending order

Source: https://exaly.com/author-pdf/5098671/publications.pdf Version: 2024-02-01



#	Article	IF	CITATIONS
1	Deterministic Shallow Dopant Implantation in Silicon with Detection Confidence Upperâ€Bound to 99.85% by Ion–Solid Interactions. Advanced Materials, 2022, 34, e2103235.	11.1	16
2	Deterministic Shallow Dopant Implantation in Silicon with Detection Confidence Upperâ€Bound to 99.85% by Ion–Solid Interactions (Adv. Mater. 3/2022). Advanced Materials, 2022, 34, .	11.1	1
3	Properties of gallium oxide thin films grown by ion beam sputter deposition at room temperature. Journal of Vacuum Science and Technology A: Vacuum, Surfaces and Films, 2022, 40, .	0.9	2
4	Image charge detection of ion bunches using a segmented, cryogenic detector. Journal of Applied Physics, 2022, 131, .	1.1	4
5	Vacancy diffusion and nitrogen-vacancy center formation near the diamond surface. Applied Physics Letters, 2021, 118, .	1.5	9
6	Characterization of an RF excited broad beam ion source operating with inert gases. Journal of Applied Physics, 2021, 129, .	1.1	5
7	Toward a systematic discovery of artificial functional magnetic materials. Physical Review B, 2021, 104,	1.1	5
8	Defectâ€Induced Magnetism in Nonmagnetic Oxides: Basic Principles, Experimental Evidence, and Possible Devices with ZnO and TiO <sub>2</sub> . Physica Status Solidi (B): Basic Research, 2020, 257, 1900623.	0.7	26
9	Titanium 3d ferromagnetism with perpendicular anisotropy in defective anatase. Physical Review B, 2020, 101, .	1.1	10
10	Nanoscale ion implantation using focussed highly charged ions. New Journal of Physics, 2020, 22, 083028.	1.2	10
11	Image charge detection statistics relevant for deterministic ion implantation. Journal Physics D: Applied Physics, 2019, 52, 305103.	1.3	11
12	Ion beam sputter deposition of TiO2 films using oxygen ions. European Physical Journal B, 2018, 91, 1.	0.6	10
13	Detection of small bunches of ions using image charges. Scientific Reports, 2018, 8, 9781.	1.6	26
14	Graphene on silicon dioxide via carbon ion implantation in copper with PMMA-free transfer. Applied Physics Letters, 2017, 110, .	1.5	4
15	Advanced Electric Propulsion Diagnostic Tools at IOM. Procedia Engineering, 2017, 185, 1-8.	1.2	3
16	Modelling of a radio frequency plasma bridge neutralizer (RFPBN). Procedia Engineering, 2017, 185, 9-16.	1.2	6
17	Systematic investigation of the properties of TiO2 films grown by reactive ion beam sputter deposition. Applied Surface Science, 2017, 421, 331-340.	3.1	37
18	Strong out-of-plane magnetic anisotropy in ion irradiated anatase TiO2 thin films. AIP Advances, 2016, 6, 125009.	0.6	16

#	Article	IF	CITATIONS
19	Identification of a possible superconducting transition above room temperature in natural graphite crystals. New Journal of Physics, 2016, 18, 113041.	1.2	51
20	Evidence for Magnetic Order in Graphite from Magnetization and Transport Measurements. Springer Series in Materials Science, 2016, , 45-76.	0.4	4
21	Local zincblende coordination in heteroepitaxial wurtzite Zn1â^²xMgxO:Mn thin films with 0.01 ≤ ≤ 0.04 identified by electron paramagnetic resonance. Journal of Materials Chemistry C, 2015, 3, 11918-11929.	2.7	2
22	Magnetic order and superconductivity observed in bundles of double-wall carbon nanotubes. Carbon, 2015, 88, 16-25.	5.4	24
23	Topological insulator thin films starting from the amorphous phase-Bi2Se3as example. Journal of Applied Physics, 2015, 117, 075301.	1.1	16
24	Single atom devices by ion implantation. Journal of Physics Condensed Matter, 2015, 27, 154204.	0.7	61
25	Study of the negative magneto-resistance of single proton-implanted lithium-doped ZnO microwires. Journal of Physics Condensed Matter, 2015, 27, 256002.	0.7	8
26	Trace element content and magnetic properties of commercial HOPG samples studied by ion beam microscopy and SQUID magnetometry. AIP Advances, 2014, 4, 107142.	0.6	23
27	Silicide induced ion beam patterning of Si(001). Nanotechnology, 2014, 25, 115303.	1.3	40
28	Myelin and iron concentration in the human brain: A quantitative study of MRI contrast. NeuroImage, 2014, 93, 95-106.	2.1	528
29	A quantitative study of the intracellular concentration of graphene/noble metal nanoparticle composites and their cytotoxicity. Nanoscale, 2014, 6, 8535-8542.	2.8	66
30	Local lattice distortions in oxygen deficient Mn-doped ZnO thin films, probed by electron paramagnetic resonance. Journal of Materials Chemistry C, 2014, 2, 4947.	2.7	30
31	Defect-Induced Magnetism in Solids. IEEE Transactions on Magnetics, 2013, 49, 4668-4674.	1.2	87
32	Defect-induced magnetism in homoepitaxial manganese-stabilized zirconia thin films. Journal Physics D: Applied Physics, 2013, 46, 275002.	1.3	17
33	Comment on "Revealing common artifacts due to ferromagnetic inclusions in highly oriented pyrolytic graphite―by Sepioni M. et al Europhysics Letters, 2012, 98, 57006.	0.7	12
34	Electrical transport in strained Mg <sub><i>x</i></sub> Zn <sub>1â^'<i>x</i></sub> O:P thin films grown by pulsed laser deposition on ZnO(000â€1). Physica Status Solidi (B): Basic Research, 2012, 249, 82-90.	0.7	4
35	Hydrogen-mediated ferromagnetism in ZnO single crystals. New Journal of Physics, 2011, 13, 063017.	1.2	40
36	Materials analysis and modification at LIPSION – Present state and future developments. Nuclear Instruments & Methods in Physics Research B, 2011, 269, 2175-2179.	0.6	20

#	Article	lF	CITATIONS
37	Magnetic order in graphite: Experimental evidence, intrinsic and extrinsic difficulties. Journal of Magnetism and Magnetic Materials, 2010, 322, 1156-1161.	1.0	48
38	The role of hydrogen in room-temperature ferromagnetism at graphite surfaces. New Journal of Physics, 2010, 12, 123012.	1.2	101
39	Low-energy and SQUID evidence of magnetism in highly oriented pyrolytic graphite. Journal of Magnetism and Magnetic Materials, 2010, 322, 1228-1231.	1.0	11
40	Magnetic order in proton irradiated graphite: Curie temperatures and magnetoresistance effect. Journal of Nuclear Materials, 2009, 389, 336-340.	1.3	9
41	Defect-induced magnetic order in pure ZnO films. Physical Review B, 2009, 80, .	1.1	274
42	The influence of iron, fluorine and boron implantation on the magnetic properties of graphite. Journal of Magnetism and Magnetic Materials, 2008, 320, 966-977.	1.0	23
43	Creation of GaAs microstructures using the nuclear nanoprobe LIPSION. Semiconductor Science and Technology, 2008, 23, 125028.	1.0	8
44	Experimental evidence for two-dimensional magnetic order in proton bombarded graphite. Physical Review B, 2007, 76, .	1.1	112
45	Ï€-Electron Ferromagnetism in Metal-Free Carbon Probed by Soft X-Ray Dichroism. Physical Review Letters, 2007, 98, 187204.	2.9	258
46	Electrical and magnetic properties of RE-doped ZnO thin films (RE = Gd, Nd). Superlattices and Microstructures, 2007, 42, 231-235.	1.4	71
47	Possible pitfalls in search of magnetic order in thin films deposited on single crystalline sapphire substrates. Journal of Magnetism and Magnetic Materials, 2007, 317, 53-60.	1.0	40
48	Optical and structural properties of MgZnO/ZnO hetero- and double heterostructures grown by pulsed laser deposition. Applied Physics A: Materials Science and Processing, 2007, 88, 99-104.	1.1	31
49	Electronic band gap of Zn2x(CuIn)1â^'xX2 solid solution series (X=S, Se, Te). Journal of Alloys and Compounds, 2006, 414, 26-30.	2.8	42
50	Growth of highly oriented graphite films at room temperature by pulsed laser deposition using carbon–sulfur targets. Carbon, 2006, 44, 3064-3072.	5.4	17
51	Room-temperature ferromagnetic Mn-alloyed ZnO films obtained by pulsed laser deposition. Journal of Magnetism and Magnetic Materials, 2006, 307, 212-221.	1.0	38
52	Deep defects generated in n-conducting ZnO:TM thin films. Solid State Communications, 2006, 137, 417-421.	0.9	14
53	Proton irradiation effects and magnetic order in carbon structures. Thin Solid Films, 2006, 505, 85-89.	0.8	10
54	Magnetoresistance in pulsed laser deposited 3d transition metal doped ZnO films. Thin Solid Films, 2006, 515, 2549-2554.	0.8	20

#	Article	IF	CITATIONS
55	Weak ferromagnetism in textured Zn1â^'x(TM)xO thin films. Superlattices and Microstructures, 2006, 39, 334-339.	1.4	14
56	Refractive indices and band-gap properties of rocksalt MgxZn1â^'xO (0.68⩽x⩽1). Journal of Applied Physi 2006, 99, 123701.	<sup>CS</sup> .1	55
57	Magnetism in Carbon: Writing Magnetic Structures with a Proton Micro-Beam on Graphite Surfaces. Acta Physica Polonica A, 2006, 109, 249-255.	0.2	1
58	Morphological and elemental characterisation with the high-energy ion-nanoprobe LIPSION. Applied Surface Science, 2005, 252, 43-48.	3.1	8
59	The two-phase region in 2(ZnSe)x(CuInSe2)1â^'x alloys and structural relation between the tetragonal and cubic phases. Journal of Solid State Chemistry, 2005, 178, 3631-3638.	1.4	21
60	UV optical properties of ferromagnetic Mn-doped ZnO thin films grown by PLD. Thin Solid Films, 2005, 486, 117-121.	0.8	66
61	The Role of Nuclear Nanoprobes in Inducing Magnetic Ordering in Graphite. Hyperfine Interactions, 2005, 160, 27-37.	0.2	5
62	BIOMEDICAL IMAGING WITH THE LEIPZIG HIGH-ENERGY ION-NANOPROBE LIPSION. International Journal of PIXE, 2005, 15, 125-130.	0.4	0
63	Examples of room-temperature magnetic ordering in carbon-based structures. Phase Transitions, 2005, 78, 155-171.	0.6	10
64	MgxZn1â^'xO(0⩽x<0.2) nanowire arrays on sapphire grown by high-pressure pulsed-laser deposition. Applied Physics Letters, 2005, 86, 143113.	1.5	188
65	Magnetic carbon: Explicit evidence of ferromagnetism induced by proton irradiation. Carbon, 2004, 42, 1213-1218.	5.4	49
66	Ion-beam analysis of CuInSe2 solar cells deposited on polyimide foil. Analytical and Bioanalytical Chemistry, 2004, 379, 622-7.	1.9	7
67	Lattice parameter and elastic constants of cubic Zn1â~'x Mn x Se epilayers grown by molecular-beam epitaxy. Physica Status Solidi C: Current Topics in Solid State Physics, 2004, 1, 649-652.	0.8	15
68	Intrinsic carbon doping of (AlGa)As for (InGa)As laser structures (λâ‰^1.17μm). Journal of Crystal Growth, 2004, 272, 642-649.	0.7	3
69	Infrared dielectric function and phonon modes of Mg-rich cubic MgxZn1â^'xO(x⩾0.67) thin films on sapphire (0001). Applied Physics Letters, 2004, 85, 905-907.	1.5	29
70	Induced Magnetic Ordering by Proton Irradiation in Graphite. Physical Review Letters, 2003, 91, 227201.	2.9	759
71	Ferromagnetic Spots in Graphite Produced by Proton Irradiation. Advanced Materials, 2003, 15, 1719-1722.	11.1	140
72	Observation of intrinsic magnetic domains in C60 polymer. Carbon, 2003, 41, 785-795.	5.4	69

#	Article	IF	CITATIONS
73	Addendum to "Observation of intrinsic magnetic domains in C60 polymers― Carbon, 2003, 41, 2425-2426.	5.4	18
74	Dielectric properties of Fe-doped BaxSr1â^xTiO3 thin films on polycrystalline substrates at temperatures between â^'35 and +85 °C. Solid-State Electronics, 2003, 47, 2199-2203.	0.8	24
75	Optical and electrical properties of epitaxial (Mg,Cd)xZn1â^'xO, ZnO, and ZnO:(Ga,Al) thin films on c-plane sapphire grown by pulsed laser deposition. Solid-State Electronics, 2003, 47, 2205-2209.	0.8	140
76	Infrared dielectric functions and phonon modes of high-quality ZnO films. Journal of Applied Physics, 2003, 93, 126-133.	1.1	590
77	Dielectric functions (1 to 5 eV) of wurtzite MgxZn1â^'xO (x⩼20.29) thin films. Applied Physics Letters, 2003 82, 2260-2262.	'1.5	165
78	Raman scattering in ZnO thin films doped with Fe, Sb, Al, Ga, and Li. Applied Physics Letters, 2003, 83, 1974-1976.	1.5	595
79	Infrared dielectric functions and phonon modes of wurtzite MgxZn1â^xOâ€,(x⩽0.2). Applied Physics Letters, 2002, 81, 2376-2378.	1.5	65
80	Ferromagnetism in oriented graphite samples. Physical Review B, 2002, 66, .	1.1	352
81	Non-destructive 3D-characterization of Zn 2-2x Cu x In x S 2 -thin films with ion beam analysis. Analytical and Bioanalytical Chemistry, 2002, 374, 626-630.	1.9	1
82	The Leipzig high-energy ion nanoprobe: A report on first results. Nuclear Instruments & Methods in Physics Research B, 2000, 161-163, 323-327.	0.6	52
83	Solid State Analysis with the New Leipzig High-Energy Ion Nanoprobe. Mikrochimica Acta, 2000, 133, 105-111.	2.5	18
84	Combination of Micro-PIXE with the Pattern Recognition Technique for the Source Identification of Individual Aerosol Particles. Applied Spectroscopy, 2000, 54, 807-811.	1.2	10
85	Source Identification of Lead Pollution in the Atmosphere of Shanghai City by Analyzing Single Aerosol Particles (SAP). Environmental Science & Technology, 2000, 34, 1900-1905.	4.6	51